Research

Tracking dragons: stable isotopes reveal the annual cycle of a long-distance migratory insect

Michael T. Hallworth[1,2], Peter P. Marra[1], Kent P. McFarland[3], Sara Zahendra[3] and Colin E. Studds[1,2]

[1]Migratory Bird Center, Smithsonian Conservation Biology Institute, Washington, DC 20008, USA
[2]Department of Geography and Environmental Systems, University of Maryland, Baltimore County, Baltimore, MD 21250, USA
[3]Vermont Center for Ecostudies, White River Junction, VT 05001, USA

MTH, 0000-0002-6385-3815; PPM, 0000-0002-0508-7577; KPM, 0000-0001-7809-5503; CES, 0000-0001-5715-1692

Insect migration is globally ubiquitous and can involve continental-scale movements and complex life histories. Apart from select species of migratory moths and butterflies, little is known about the structure of the annual cycle for migratory insects. Using stable-hydrogen isotope analysis of 852 wing samples from eight countries spanning 140 years, combined with 21 years of citizen science data, we determined the full annual cycle of a large migratory dragonfly, the common green darner (*Anax junius*). We demonstrate that darners undertake complex long-distance annual migrations governed largely by temperature that involve at least three generations. In spring, the first generation makes a long-distance northbound movement (further than 650 km) from southern to northern range limits, lays eggs and dies. A second generation emerges and returns south (further than 680 km), where they lay eggs and die. Finally, a third resident generation emerges, reproducing locally and giving rise to the cohort that migrates north the following spring. Since migration timing and nymph development are highly dependent on temperature, continued climate change could lead to fundamental changes in the biology for this and similar migratory insects.

1. Introduction

Insects are the most species-rich and abundant group of macroscopic organisms on the planet, yet our understanding of the biological underpinnings of their annual cycles and migratory behaviours drastically trails behind that of vertebrate taxa [1]. Perhaps the best-known insect migrations are the multigenerational migrations of the monarch butterfly (*Danaus plexippus*) in eastern North America [2], and the painted lady (*Vanessa cardui*) in Europe [3], which migrate southbound each autumn from the northern reaches of their distribution into southern North America and Africa, respectively. Monarchs wait out the boreal winter [4] and the same individuals migrate northbound the following spring into the southern parts of their distribution where they lay eggs, beginning the next generation that continues the northbound progression of their lifecycle [2,3,5,6].

Few migratory insects have had their full annual cycles sufficiently described despite their profound cultural [7], ecological [8] and agricultural importance [9]. This disparity is owing largely to the difficulties with tracking small organisms over space and time, as well as their complex life histories that often require both terrestrial and aquatic habitats [10]. Among the migratory

insects, almost all are suspected to employ complex multi-generational migrations (but see [7,8]) similar to the monarch butterfly and painted lady, where no single individual completes the entire migratory circuit [2,3,5,6,10,11]. The continental distances travelled [12,13], small body sizes and multi-generational aspect of their life histories pose significant challenges to understanding the fundamental biology of the full annual cycles of migratory insects. Adding to this complexity, movements, timing and life-history strategies are likely linked to photoperiod, weather, temperature and other environmental forces [1,3,11,14–16].

The common green darner (*Anax junius*) is a ubiquitous, charismatic migratory dragonfly found in North America. Its complex life-history includes both resident and migratory populations. The aquatic nymphs likely give rise to resident and migratory phenotypes because they exhibit two distinct developmental strategies [14]. Nymphs either undergo rapid development and emerge within a single season or develop slowly, enter diapause and emerge the following summer [14]. The developmental strategy is governed by the photoperiod experienced by the egg or early instars [17] and temperature [14]. Therefore, the seasonal timing of oviposition likely determines whether nymphs develop, emerge within a single growing season and migrate, or enter diapause.

Darner migration is considered an adaptive strategy because it spreads reproductive effort across multiple, widely separated water bodies and ameliorates the risk of predation, competition and drought [17,18]. Migratory movements are commonly observed in autumn and have been documented using direct [12] and indirect techniques [19]. Northbound migration in spring is suspected and supported by anecdotal observations but is not well documented [20]. Although it is known that common green darners migrate, no study to date has linked multiple populations over time and space to better understand the phenology of the annual cycle and the number of generations involved.

2. Methods and materials

We combined observational and stable-hydrogen isotope data to identify the timing of migration and emergence origins of darners. Two publicly available datasets were assembled to refine emergence assignments using stable isotopes. First, we acquired citizen science data on the first observed migratory adult common green darners (first flight dates) to determine the minimum temperature necessary for darners to migrate (electronic supplementary material, table S1). Daily mean temperature of the first flight date was 9.17°C, similar to the development threshold (8.7 ± 0.1°C) reported by Trottier [14]. In addition to determining the temperature threshold for migratory flights, we used occurrence records submitted by citizen scientists and museum collections to generate a habitat suitability surface that we included as prior information in the probabilistic isotope-assignments [21] (see §2a).

(a) Emergence assignments

We obtained contemporary and museum specimens from 681 locations from eight countries ranging from the tropics to the northern temperate zone (17.98° N to 51.14° N) that we used to describe migration phenology and the number of generations within the annual cycle for the common green

darner. Specimens, which included exuviae, tenerals and mature adults, were collected in every calendar month spanning over 100 years (electronic supplementary material, table S2). Isotope analyses were performed on a small distal segment of the wing to determine where the captured individuals emerged (see electronic supplementary material).

(b) Migratory distance

Determining the exact emergence origin from stable isotopes is not possible given the uncertainty in geographical assignment and lack of longitudinal variation in the underlying isoscape. Therefore, we used a conservative distance estimator as an index of migration distance. We determined the minimum distance (kilometres) between the 'likely' emergence origin surface and the location where the specimen was collected (i.e. shortest possible distance travelled). Migration distances were calculated using the gDistance function in the rgeos [22] package in program R [23].

(c) Annual cycle

We summarized the emergence origins within the hardiness zones (see electronic supplementary material, delineating populations) for each calendar month to describe the phenology of the annual cycle. Isotope-based emergence origins provide spatio-temporal information of adults but the phenology of nymph development and emergence timing is also needed to fully understand the annual cycle of darners.

3. Results

We combined data on stable-hydrogen isotopes of 852 common green darner museum and contemporary specimens spanning 140 years (1874–2013) from eight countries with citizen science observations to determine the emergence origin, continental migrations and annual cycle of the common green darner. Using citizen science observations, we found that northbound darner migration closely tracks a thermocline of 9.17°C (figure 1). We then used this temperature-dependent flight phenology to refine stable-isotope assignments, and found that adults originating from the southern range margin migrate a minimum of 659.46 ± 49.11 km to the northern range edge in March and April ($n = 50$; electronic supplementary material, figure S1a). Previous estimates of darner daily migration rates indicate this journey would take 55.42 ± 4.13 days to complete [12]. Therefore, the first migratory individuals arriving in the north likely emerge in the south in January and February. However, prevailing wind patterns in spring favour northbound migration, potentially allowing individuals to migrate faster [24]. If darners use high-altitude migratory flights to take advantage of fast-moving winds, the distances reported above could be covered more rapidly [11,13,25].

Combining stable-isotope assignments and temperature-related nymph development [14], we found the annual cycle of common green darners is comprised of at least three generations (figure 2). The first generation emerges between January and May in the southern part of the distribution and migrates north into the northern reaches of the distribution. The first generation is complete by August, the last month when darners with southern stable isotopic origins are captured in the north (figure 2, August). The first
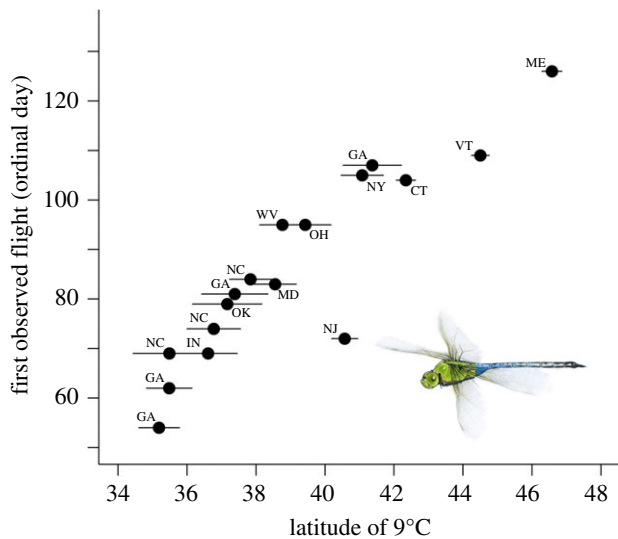
Figure 1. First flight date of adult common green darner and the latitude of the 9.17°C thermocline. The mean latitude of the thermocline was extracted along the observation longitude from 1994 to 2014. Error bars represent the standard error in the latitude of the thermocline on the first flight date. Data represented in figure 1 can be found in electronic supplementary material, table S1. Graphic was drawn by Matthew Dodder (https://neornithes.wordpress.com) and used with permission. (Online version in colour.)

cohort of the second generation—young from the previous year that overwinter as late-stage instars and eclose between May and July [14]—begin flying in May with 4% (2 of 53; figure 2, May) of individuals assigned to where they were captured. Spatio-temporal overlap exists between the first and second generations as northbound migration continues through July. The number of locally emerged darners in the north increases throughout the season, peaking in September when offspring of the first generation in April and early May eclose (May: 4%, 2 of 53; June: 22%, 16 of 74; July: 29%, 15 of 52; August: 50%, 5 of 10; September: 86%, 6 of 7; October: 67%, 2 of 3; electronic supplementary material, figure S3). This latter cohort of the second generation then migrates south.

Second generation darners with northern isotopic signatures are first detected in the south during August and September (figure 2, September), suggesting southbound migration begins in July and continues into October [12]. These southbound migrants are composed of darners that overwinter as nymphs and emerge in June and July and darners who develop within a single growing season that eclose in September. Southbound migration to the southern range edge peaks in September and October, with 64% (7 of 11) of green darners captured at least 680.97 ± 178.84 km from where they emerge in the north (electronic supplementary material, figure S1b). The second generation composed of individuals that emerge in the northern portion of the distribution ends in late October (figure 2, October). After this time, no individuals with northern isotopic signatures were captured in the south (figure 2, November), suggesting they die shortly after they arrive in the south. However, southbound migrants from mid-latitudes were captured in November (43%, 3 of 7; figure 2, November) and December (57%, 4 of 7), emerging a minimum of 226.13 ± 108.50 and 232.03 ± 93.28 km away from where they were captured, respectively. A third, non-migratory generation occurs in the

south between November and January (figure 2, November–January). This generation must be resident because adults that emerge in November likely die before April and May when the first migratory individuals are captured in the north, based on the adult longevity reported for the species (five to seven weeks [16]). Thus, third generation adults that emerge in November likely give rise to the first generation of migratory individuals that are captured in the north. Stable isotopes, however, are unable to differentiate between the first and proposed third generation.

4. Discussion

The annual cycle of green darners is composed of at least two migratory and one non-migratory generations. In spring, the first generation makes a long-distance northbound movement (659.46 ± 49.11 km) from southern to northern range limits, lays eggs and dies. A second generation emerges and returns south (680.97 ± 178.84 km), where they lay eggs and die. Finally, a third resident generation emerges, reproducing locally and giving rise to the cohort that migrates north the following spring.

During spring, individuals with southern emergence origins arrive at northern locations prior to those with origins from mid-latitudes (electronic supplementary material, figure S2). A similar pattern is observed in autumn, where individuals with northern origins are captured in the southern portion of their distribution before green darners that emerge at mid-latitudes. This migratory phenomenon could arise from several alternative life-history strategies. First, such patterns could result if individuals spread reproductive risk across multiple, widely separated water bodies and reproduce during their migratory journey north [18]. Their offspring could take advantage of warm surface waters, mature rapidly within the same growing season and migrate northbound (electronic supplementary material, figure S4). Such a strategy is akin to the multi-generational migration of the monarch and painted lady butterflies [1,2], however, the longevity and strong direct flights of darners allow populations to be connected over larger spatial scales compared to the northbound multi-generational progression of migratory butterflies. The observed pattern of shortened migratory distances as the season progresses also could result if individuals reproduce during southbound migration. If darners reproduce during the journey south, their eggs would hatch but the nymphs would enter a state of diapause as temperatures drop, emerge and migrate north the following spring when suitable thermal conditions allow [14,18]. A combination of these strategies is likely. Plasticity in nymph development further complicates discerning between the two strategies. Eggs laid during migratory periods could either (i) undergo rapid development after hatching and emerge within the same season or (ii) hatch, enter diapause as nymphs and emerge the following spring, depending on the photoperiod experienced by the egg or early instar [17]. Stable-hydrogen isotope data cannot differentiate between these competing hypotheses. Regardless of the strategy, the timing of migratory movements allows for spatial and temporal overlap of both migratory and non-migratory populations, explaining the lack of genetic structure in this species [18,26].
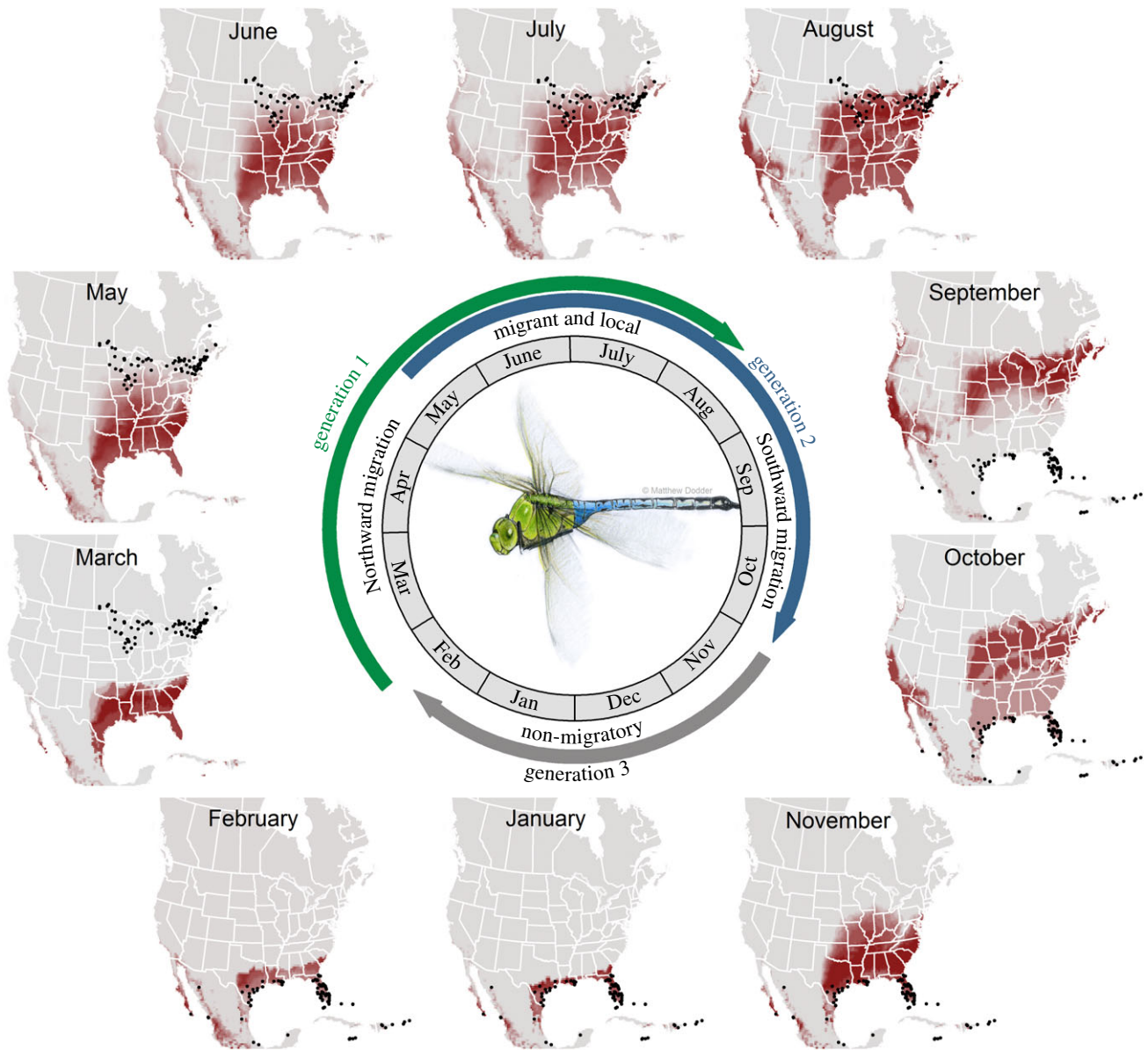
Figure 2. The full annual cycle of the common green darner is comprised of three generations. The first generation is migratory, emerges in the south between February and May and dies in the north. The second generation emerges in the north, migrates south and dies. The third generation, offspring of migratory individuals in the fall, is non-migratory and emerges in the south in November. The emergence origins of adults (colour ramp; grey = zero, red = many) captured at the sampling locations (black dots) in each month are shown around the perimeter. Graphic was drawn by Matthew Dodder (https://neornithes.wordpress.com) and used with permission.

Common green darner migration appears to be governed in part by temperature. Northbound adult migration during spring coincides with a daily mean thermocline of approximately 9°C (9.17°C) and the last observed adults in autumn coincide with a similar thermocline (9.54°C). These findings are consistent with the short migratory movements of tagged individuals following synoptic cold fronts [12]. In addition, the 9°C thermocline observed here is similar to the development threshold of the final instar (8.7 ± 0.1°C) [14]. Taken together, these findings suggest that temperature is a key limiting factor to the northbound migration of dragonflies in spring, the emergence of nymphs and southbound migration in autumn. Given the critical role of temperature, a warming climate could induce earlier spring flights, trigger later autumn flights and potentially shorten migratory distances as the 9°C thermocline moves northbound, allowing adults to reside at higher latitudes during the winter months. Further research is needed to determine how a changing climate may alter the migratory schedules and annual cycle of dragonflies and other migratory insects.

References

1. Chapman JW, Reynolds DR, Wilson K. 2015 Long-range seasonal migration in insects: mechanisms, evolutionary drivers and ecological consequences. *Ecol. Lett.* **18**, 287–302. (doi:10.1111/ele.12407)

2. Flockhart DTT, Wassenaar LI, Martin TG, Hobson KA, Wunder MB, Norris DR. 2013 Tracking multi-generational colonization of the breeding grounds by monarch butterflies in eastern North America. *Proc. R. Soc. B* **280**, 20131087. (doi:10.1098/rspb.2013.1087)

3. Stefanescu C et al. 2013 Multi-generational long-distance migration of insects: studying the painted lady butterfly in the Western Palaearctic. *Ecography* **36**, 474–486. (doi:10.1111/j.1600-0587.2012.07738.x)

4. Wassenaar LI, Hobson KA. 1998 Natal origins of migratory monarch butterflies at wintering colonies in Mexico: new isotopic evidence. *Proc. Natl Acad. Sci. USA* **95**, 15 436–15 439. (doi:10.1073/pnas.95.26.15436)

5. Miller NG, Wassenaar LI, Hobson KA, Norris DR. 2012 Migratory connectivity of the monarch butterfly (*Danaus plexippus*): patterns of spring re-colonization in Eastern North America. *PLoS ONE* **7**, e31891. (doi:10.1371/journal.pone.0031891)

6. Talavera G, Bataille C, Benyamini D, Gascoigne-Pees M, Vila R. 2018 Round-trip across the Sahara: Afrotropical painted lady butterflies recolonize the Mediterranean in early spring. *Biol. Lett.* **14**, 20180274. (doi:10.1098/rsbl.2018.0274)

7. Common IFB. 1954 A study of the ecology of the adult bogong moth, *Agrotis infusa* (Boisd) (Lepidoptera: Noctuidae), with special reference to its behaviour during migration and aestivation. *Aust. J. Zool.* **2**, 223–263. (doi:10.1071/zo9540223)

8. Warrant E, Frost B, Green K, Mouritsen H, Dreyer D, Adden A, Brauburger K, Heinze S. 2016 The Australian bogong moth *Agrotis infusa*: a long-distance nocturnal navigator. *Front. Behav. Neurosci.* **10**, 77. (doi:10.3389/fnbeh.2016.00077)

9. Nagoshi RN, Meagher RL, Hay-Roe M. 2012 Inferring the annual migration patterns of fall armyworm (Lepidoptera: Noctuidae) in the United States from mitochondrial haplotypes. *Ecol. Evol.* **2**, 1458–1467. (doi:10.1002/ece3.268)

10. Alerstam T, Chapman JW, Backman J, Smith AD, Karlsson H, Nilsson C, Reynolds DR, Klaassen RHG, Hill JK. 2011 Convergent patterns of long-distance nocturnal migration in noctuid moths and passerine birds. *Proc. R. Soc. B* **278**, 3074–3080. (doi:10.1098/rspb.2011.0058)

11. Anderson RC. 2009 Do dragonflies migrate across the western Indian Ocean? *J. Trop. Ecol.* **25**, 347–358. (doi:10.1017/S0266467409006087)

12. Wikelski M, Moskowitz D, Adelman JS, Cochran J, Wilcove DS, May ML. 2006 Simple rules guide dragonfly migration. *Biol. Lett.* **2**, 325–329. (doi:10.1098/rsbl.2006.0487)

13. Hobson KA, Anderson RC, Soto DX, Wassenaar LI. 2012 Isotopic evidence that dragonflies (*Pantala flavescens*) migrating through the Maldives come from the Northern Indian subcontinent. *PLoS ONE* **7**, e52594. (doi:10.1371/journal.pone.0052594)

14. Trottier R. 1971 Effect of temperature on the life-cycle of *Anax junius* (Odonata: Aeshnidae) in Canada. *Can. Entomol.* **103**, 1671–1683. (doi:10.4039/Ent1031671-12)

15. Corbet PS. 2014 Dragonflies: Behaviour and Ecology of Odonata. See http://www.nhbs.com/dragonflies-behaviour-and-ecology-of-odonata-book (accessed on 13 September 2017).

16. May ML. 2013 A critical overview of progress in studies of migration of dragonflies (Odonata: Anisoptera), with emphasis on North America. *J. Insect Conserv.* **17**, 1–15. (doi:10.1007/s10841-012-9540-x)

17. Matthews JH. 2007 Research in motion: patterns of large-scale migration in dragonflies and birds, pp. 62–91. PhD Dissertation, University of Texas.

18. May ML, Gregoire JA, Gregoire SM, Lubertazzi MA, Matthews JH. 2017 Emergence phenology, uncertainty, and the evolution of migratory behavior in *Anax junius* (Odonata: Aeshnidae). *PLoS ONE* **12**, e0183508. (doi:10.1371/journal.pone.0183508)

19. Hobson KA, Soto DX, Paulson DR, Wassenaar LI, Matthews JH. 2012 A dragonfly (δ^2H) isoscape for North America: a new tool for determining natal origins of migratory aquatic emergent insects. *Methods Ecol. Evol.* **3**, 766–772. (doi:10.1111/j.2041-210X.2012.00202.x)

20. Russell RW, May ML, Soltesz KL, Fitzpatrick JW. 1998 Massive swarm migrations of dragonflies (Odonata) in Eastern North America. *Am. Midl. Nat.* **140**, 325–342. (doi:10.1674/0003-0031(1998)140[0325:MSMODO]2.0.CO;2)

21. Andrew Royle J, Rubenstein DR. 2004 The role of species abundance in determining breeding origins of migratory birds with stable isotopes. *Ecol. Appl.* **14**, 1780–1788. (doi:10.1890/04-0175)

22. Bivand R, Rundel C, Pebesma E, Stuetz R, Hufthammer KO, Giraudoux P, Davis M, Santilli S. 2018 *rgeos: Interface to Geometry Engine - Open Source* (*GEOS*). See https://CRAN.R-project.org/package=rgeos.

23. R Core Team. 2016 *R: A language and environment for statistical computing*. Vienna, Austria: R Foundation for Statistical Computing. See https://www.R-project.org/.

24. Kranstauber B, Weinzierl R, Wikelski M, Safi K. 2015 Global aerial flyways allow efficient travelling. *Ecol. Lett.* **18**, 1338–1345. (doi:10.1111/ele.12528)

25. Feng H-Q, Wu K-M, Ni Y-X, Cheng D-F, Guo Y-Y. 2006 Nocturnal migration of dragonflies over the Bohai Sea in northern China. *Ecol. Entomol.* **31**, 511–520. (doi:10.1111/j.1365-2311.2006.00813.x)

26. Freeland JR, May M, Lodge R, Conrad KF. 2003 Genetic diversity and widespread haplotypes in a migratory dragonfly, the common green darner *Anax junius*. *Ecol. Entomol.* **28**, 413–421. (doi:10.1046/j.1365-2311.2003.00521.x)

27. Hallworth MT, Marra PP, McFarland KP, Zahendra S, Studds CE. 2018 Data from: Tracking dragons: stable isotopes reveal the annual cycle of a long-distance migratory insect. Dryad Digital Repository. (doi:10.5061/dryad.17hf071)

SUPPLEMENTAL INFORMATION

Tracking Dragons: Stable isotopes reveal the annual cycle of a long-distance migratory insect

Michael T. Hallworth[1,2,]*, Peter P. Marra[1], Kent P. McFarland[3], Sara Zahendra[3] and Colin E. Studds[1,2]

[1] Migratory Bird Center, Smithsonian Conservation Biology Institute, Washington, D.C. 20008.

[2] University of Maryland, Baltimore County, Baltimore, MD. 21250.

[3] Vermont Center for Ecostudies, White River Junction, VT. 05001

*Corresponding author

SUPPLEMENTAL METHODS

First flight temperature threshold - Daily mean temperature obtained from PRISM Gridded Climate Data[1] on the first flight date was extracted and summarized for each observation location from 1994 – 2014 which spanned the contemporary observations.

Habitat suitability - We generated a habitat suitability surface to help refine stable isotope geographic assignments. The habitat suitability surface was constructed using occurrence records obtained from Global Biodiversity Information Facility ([2], n = 5099) combined with our sampling locations (n = 1188) using Maxent [3] accessed through R [4] via the dismo [5] package (see SI for more information). Duplicate locations were removed from the dataset resulting in 4226 occurrence locations. The habitat suitability model was generated using a training dataset that encompassed 80% of the occurrence records. We withheld 20% of the data to test the accuracy of predicted suitability surface. Biologically relevant variables likely to influence common green darner habitat preferences and development were included in the Maxent model. Those included mean annual temperature, minimum temperature of the coldest month, annual precipitation, precipitation of the wettest month, precipitation of the driest month and elevation. Environmental layers were obtained from WorldClim.org accessed through the raster package [6]. The modelled habitat suitability surface fit the test data well (AUC = 0.873, Fig. S5).

Stable-isotope analysis - Isotope analyses were performed at the Smithsonian Institution's Stable Isotope Mass Spectrometry Laboratory in Suitland, MD, USA. Common green darner wings were washed with a 2:1 chloroform:methonal solution to remove surface oils and debris. Samples were placed in the lab 72h prior to processing to allow tissues to equilibrate to the local

atmosphere [7]. A small distal portion of the wing (0.350 ± 0.001, mean ± 1 SE) was removed

and packed into a silver capsule. Exuviae were prepared the same way as wings. Tissue samples

were combusted in an elemental analyzer and introduced to an isotope ratio mass spectrometer

via a Conflo IV interface. One in-house standard was run for every 5 unknowns to measure

accuracy and precision. Analytical error was minimal (2.63 ± 0.84 ‰) based on replicate

analysis of the same tissue samples (n = 110). The non-exchangeable hydrogen was determined

by linear regression with calibrated in-house keratin based standards (Caribou Hoof Keratin, -

197 ‰; Spectrum Keratin, -121.6 ‰; and Kudo Horn Keratin, -54.1 ‰)[7].

Creating a wing-scape - Locally emerged teneral and exuviae from 77 locations collected in 4

countries (Bahamas, Canada, Mexica, and United States) and 20 states were used to identify the

discrimination factor between the expected amount-weighted growing-season precipitation ($\delta^2 H_p$

, [8] and green darner wings (δH^2_w, Fig. S6.). The resulting dragonfly isoscape was used to

determine the origin of emergence for dragonflies collected throughout the year (Fig. S4).

Determining origin of emergence - Emergence assignments were conducted using a spatially

explicit normal probability density function [9], where the likelihood that each δH^2_w value, y*,

originated from a given location within the surface is

$$f(y^*|\mu_b, \sigma_b) = \frac{1}{\sqrt{2\pi\sigma_b}} exp\left[-\frac{1}{2\sigma_b^2}(y^* - \mu_b)^2\right]$$

where μ_b is the specific cell within the dragonfly isoscape and σ_b is the standard deviation (15.80

‰) of the residuals from the discrimination equation (see above). We included the habitat

suitability surface as prior information using Baye's rule in our geographic assignments. Doing

so increases the likelihood that assignments are made in areas where habitat is suitable and

decreases the likelihood of assignments being made to areas that are not suitable [9]. We truncated emergence assignments for individuals captured in the spring (January – May) to locations south of the 9.17°C isocline to ensure geographic assignments were biologically plausible. The resulting likelihood surface of emergence assignment was converted into a binary surface representing likely and unlikely natal origins following a 3:1 odds ratio [10].

Delineating populations –We categorized capture locations using United States Department of Agriculture hardiness zones (USDA 2012; http://planthardiness.ars.usda.gov) which are delineated into thermal zones (5.55°C) based on the average annual minimum temperature. We grouped capture locations that fell within hardiness zones 5-7 and zones 11-14 to increase the sample size in the northern and southern reaches of their distribution, respectively.

Annual cycle & larval phenology - We combined the phenology of migration derived via stable-isotopes with temperature related larval growth[11] and emergence timing[12] to better understand the full annual cycle. We estimated the date of larval emergence based on the number of accumulated growing degree-days (base = 8.7°C[11]) since oviposition. Our estimates of oviposition were constructed from the migration phenology of adults. We assumed larva emerged when the accumulated growing degree-days surpassed 1346[11]. Degree-day accumulation was derived from daily temperature minima and maxima from 1994-2014. Surface temperature was used as a proxy for surface water temperatures. Spatial-explicit daily temperature estimates were obtained from PRISM Gridded Climate Data[1].

SUPPLEMENTAL REFERENCES:

1. 2018 PRISM Climate Group, Oregon State University, http://prism.oregonstate.edu.

2. GBIF.org. 2018 GBIF Occurrence Download. See https://doi.org/10.15468/dl.pw0uol (accessed on 3 December 2018).

3. Phillips SJ, Anderson RP, Dudík M, Schapire RE, Blair ME. 2017 Opening the black box: an open-source release of Maxent. *Ecography* **40**, 887–893. (doi:10.1111/ecog.03049)

4. R Core Team. 2016 *R: A language and environment for statistical computing. R Foundation for Statistical Computing*. Vienna, Austria. See https://www.R-project.org/.

5. Hijmans RJ, Phillips S, Elith JL and J. 2017 *dismo: Species Distribution Modeling*. See https://CRAN.R-project.org/package=dismo.

6. Hijmans RJ, van Etten J. 2010 raster: Geographic analysis and modeling with raster data. *R Package Version* **1**, r948.

7. Wassenaar LI, Hobson KA. 2003 Comparative equilibration and online technique for determination of non-exchangeable hydrogen of keratins for use in animal migration studies. *Isotopes Environ. Health Stud.* **39**, 211–217.

8. Bowen GJ, Wassenaar LI, Hobson KA. 2005 Global application of stable hydrogen and oxygen isotopes to wildlife forensics. *Oecologia* **143**, 337–348.

9. Andrew Royle J, Rubenstein DR. 2004 The role of species abundance in determining breeding origins of migratory birds with stable isotopes. *Ecol. Appl.* **14**, 1780–1788.

10. Chabot AA, Hobson KA, Van Wilgenburg SL, McQuat GJ, Lougheed SC. 2012 Advances in linking wintering migrant birds to their breeding-ground origins using combined analyses of genetic and stable isotope markers. *PloS One* **7**, e43627.

11. Trottier R. 1971 Effect of temperature on the life-cycle of Anax junius (Odonata: Aeshnidae) in Canada. *Can. Entomol.* **103**, 1671–1683. (doi:10.4039/Ent1031671-12)

12. May ML, Gregoire JA, Gregoire SM, Lubertazzi MA, Matthews JH. 2017 Emergence phenology, uncertainty, and the evolution of migratory behavior in Anax junius (Odonata: Aeshnidae). *PLOS ONE* **12**, e0183508. (doi:10.1371/journal.pone.0183508)

SUPPLEMENTAL FIGURES

Fig. S1. Common green darner natal origins determined using stable-hydrogen isotopes from wings of adults flying in March and April in the northern reaches of their distribution (A) and September and October in the southern reaches of their distribution (B). The color ramps (A: gray to blue, B: gray to red) represent the number of emergence origin assignments to a particular region collected at sampling locations represented by the black dots. The minimum migration distance from the emergence origin to the collection site of each individual (A: n = 50, B: n = 11) is shown in the figure inset. Mean migration distance in spring (680.97 ± 178.84 km) and fall (659.46 ± 49.11 km) along with the standard error are indicated with the dotted red line and gray shaded area, respectively.
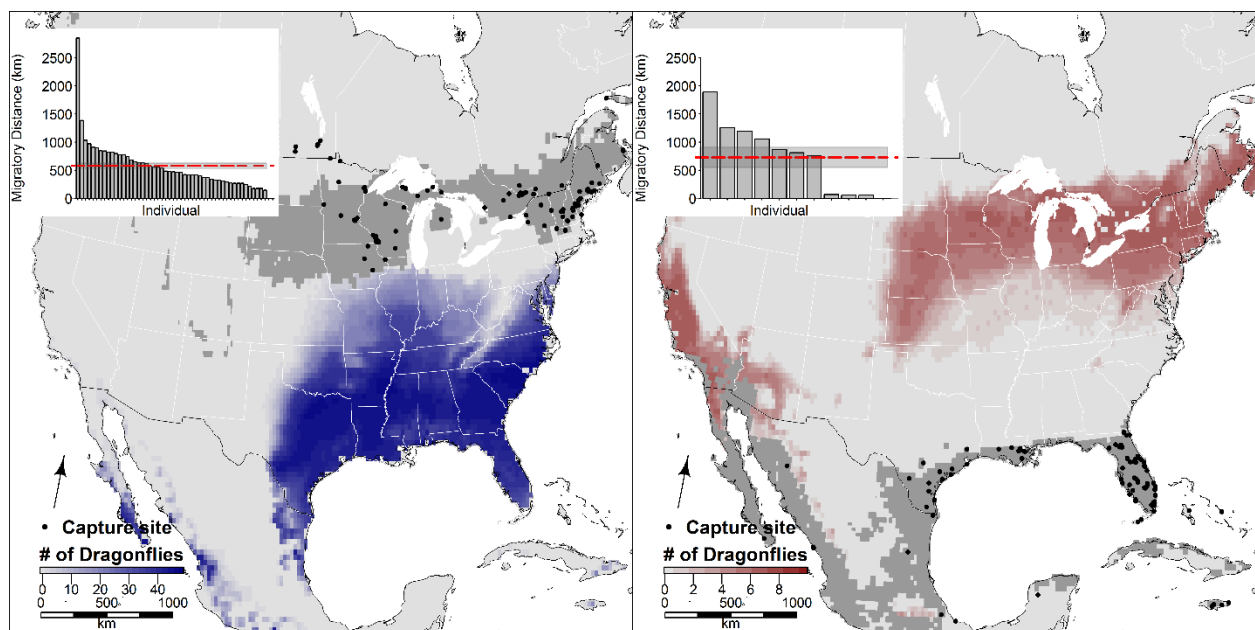
Fig. S1.

Fig. S2. Minimum migration distance between natal origin and collection site of adult common green darners flying in the northern reaches of their distribution. Adults collected in March and April were pooled to increase sample size. Individuals captured late in the season, August and September were also combined to increase sample size. The number of adults captured in each month are shown inside the each column. Figure graphic was drawn by John Muir Laws and was used with permission.
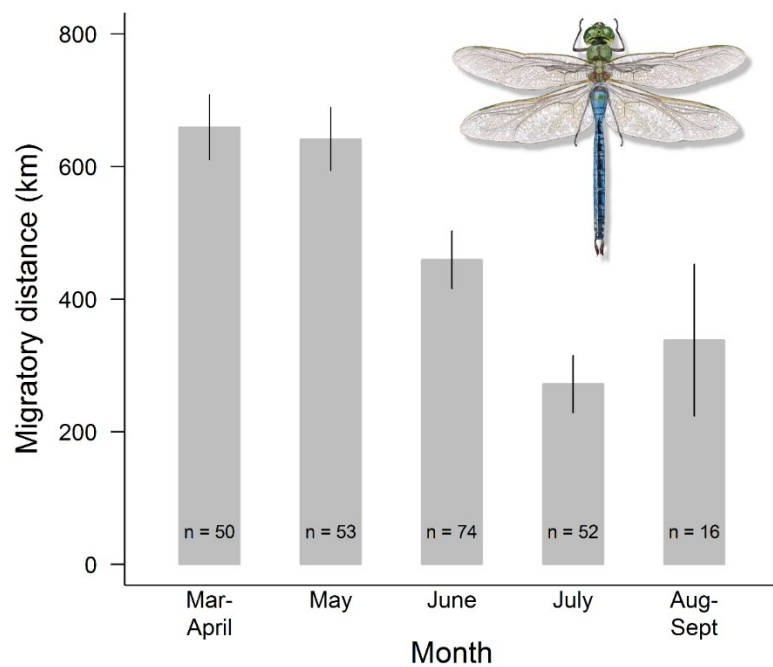
Fig. S2.

Fig. S3. Migratory status of common green darners (*Anax junius*) captured at the northern (dark gray polygon) and southern (light gray polygon) terminus of their distribution. The proportion of migratory individuals (light-blue) and locally emerged (gray) individuals sampled are shown for each month in the northern (top right) and southern (bottom right) portion of their distribution. The dotted lines and shaded polygons represent the predicted proportion and 95% confidence interval within each month, respectively. Predictions were made using a loess smoother.
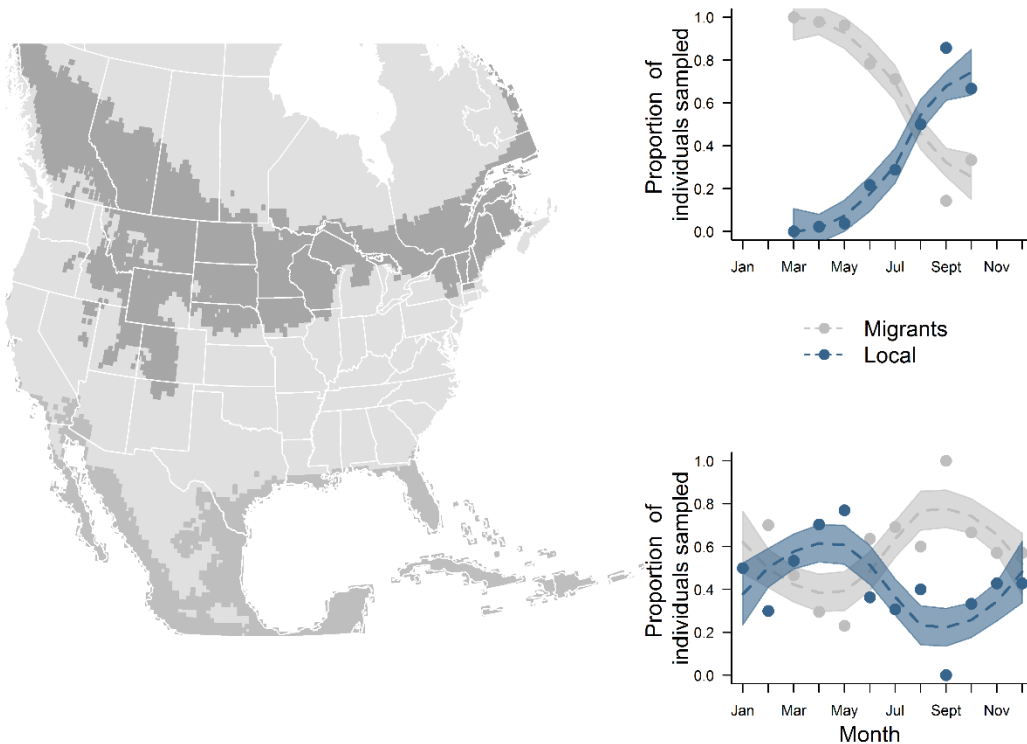
Fig. S3.

Fig. S4. Predicted common green darner (*Anax junius*) nymph development (black lines) within hardiness zones 7-11 assuming eggs are laid (black point) on the first day in each month flying adults are observed (gray boxes). Nymphs are able to eclose after accumulated growing degree days above a base of 8.7 °C reach 1346 days [10] (dotted horizontal line). Nymphs enter a state of diapause when growth is flat.
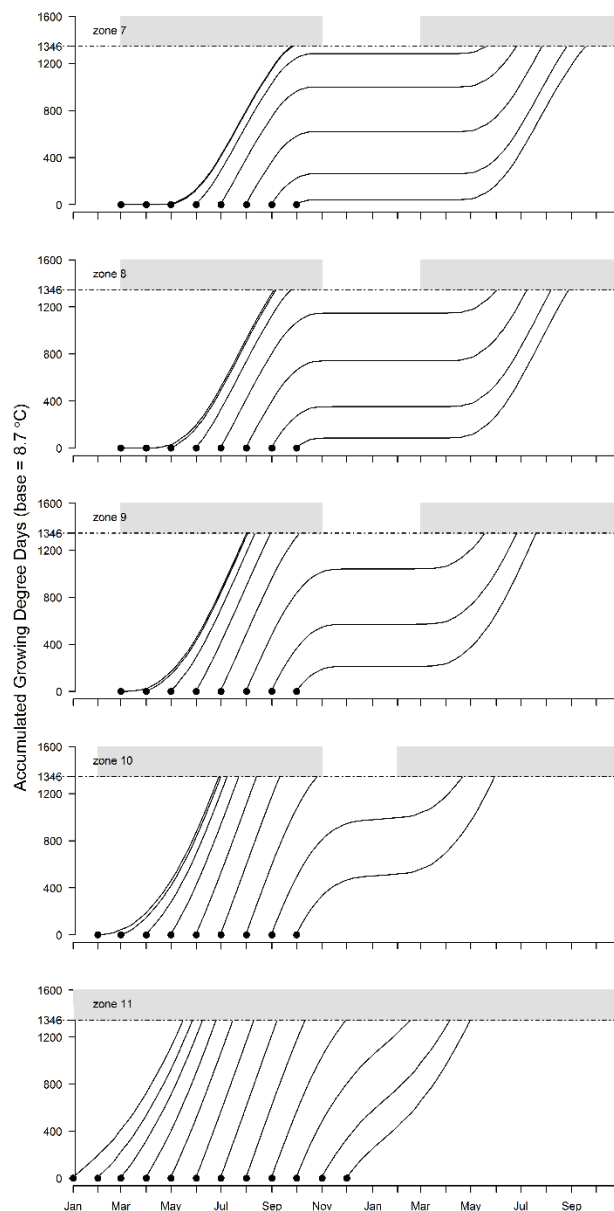
Fig. S4.

Fig. S5. Predicted habitat suitability of Common Green Darners. Habitat suitability (low

suitability = 0, high suitability = 1) of darners was derived using Maxent from occurrence

records. The area under the curve (AUC) was high indicating the predicted habitat suitability fit
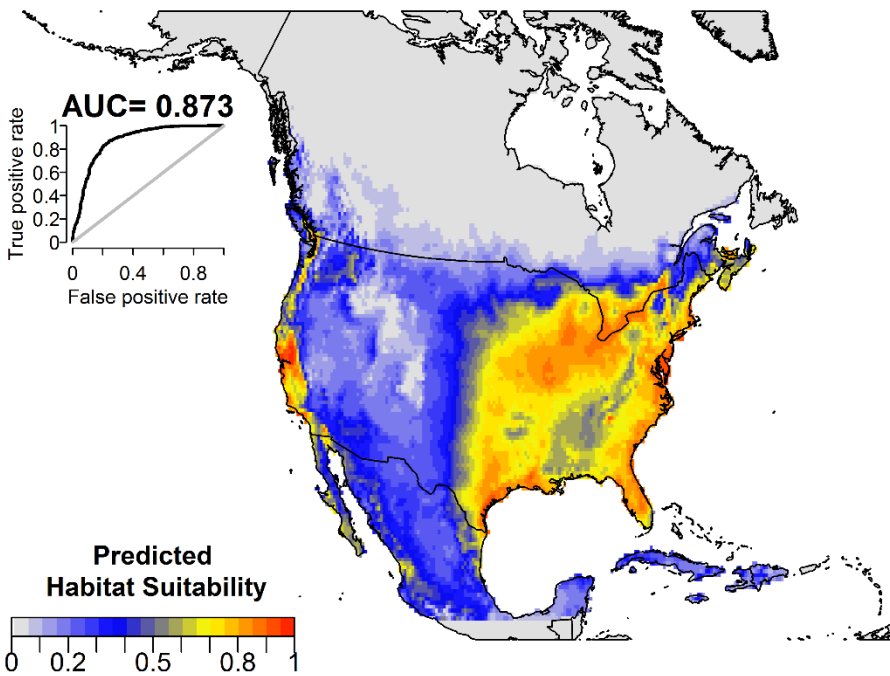
the data well.

Fig. S5

Fig. S6. Discrimination relationship between stable hydrogen isotope signatures found in amount-weighted growing-season precipitation ($\delta^2 H_{precipitation}$) and those found in local, recently emerged common green darner adults (tenerals) and exuviae ($\delta^2 H_{wing}$). This discrimination relationship was used to create a common green darner isoscape for use in assigning the natal origins to adult common green darners captured throughout their range.

Fig. S6
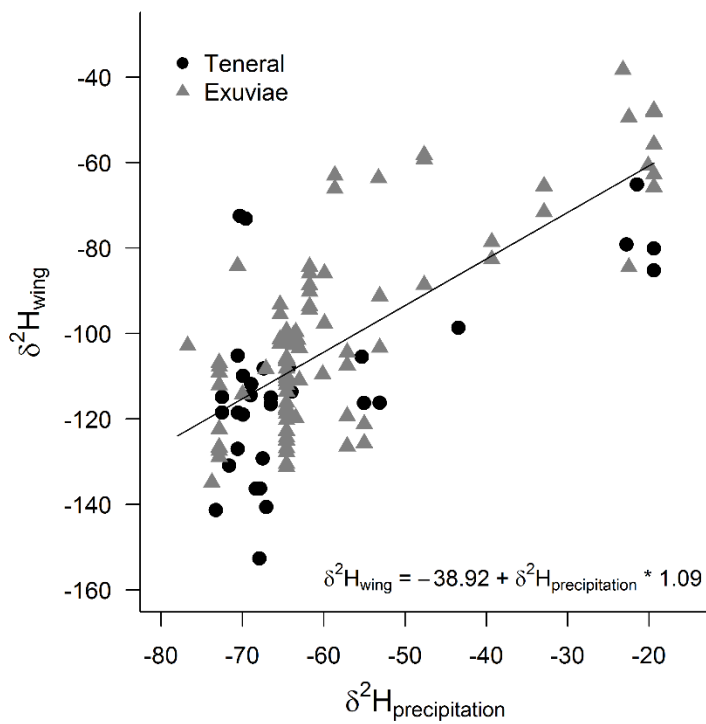
SUPPLEMENTAL TABLES

Table S1. Common green darner (*Anax junius*) survey data of first flight observations. Survey locations are indicated by the state of observation followed by the region or county where the surveys took place. If only the state is listed, surveys were conducted statewide with the exception of Maryland (MD). Surveys were conducted at the Patuxent Wildlife Research Center, in Prince George's County, Maryland. The earliest observation date (First Flight Date) represents the earliest date where an adult was observed flying in the region. The geographic coordinates of the geometric center of the state, county or location of sampling and the period covered by surveys (Years; if reported) are reported. The mean elevation of the state, county or location of sampling was determined from the SRTM 90m digital elevation model (m above sea level) accessed through the raster package[6] in program R.

Survey Location	First Flight Date	Ordinal Day	Latitude	Longitude	Years Surveyed	Elevation m. asl
GA-RV[1]	23-Feb	54	34.453	-85.015	-	263.831
GA-CP[1]	6-Mar	62	32.062	-83.008	-	84.146
IN[2]	10-Mar	69	39.920	-86.282	1900-1940	228.571
NC-M[3]	10-Mar	69	35.611	-82.785	1994-2014	923.248
NJ[4]	13-Mar	72	40.110	-74.656	2002-2006	73.708
NC-PD[3]	15-Mar	74	35.384	-80.776	1994-2014	228.481
OK[5]	20-Mar	79	36.551	-96.255	2003-2007	265.179
GA-PD[1]	22-Mar	81	33.614	-83.781	-	260.448
MD[6]	24-Mar	83	39.033	-76.809	1991-1995	62
NC-CP[3]	25-Mar	84	34.544	-78.750	1994-2014	39.684
OH[7]	5-Apr	95	40.415	-82.709	1896-1999	282.393
WV[8]	5-Apr	95	38.643	-80.614	1995-2010	510.573
CT[9]	14-Apr	104	41.575	-72.738	1999-2007	147.661
NY[10]	15-Apr	105	42.921	-75.597	2005-2009	342.287
GA-BR[1]	17-Apr	107	34.818	-84.150	-	614.035
VT[11]	19-Apr	109	44.075	-72.663	-	371.329
ME[12]	6-May	126	45.274	-69.203	1999-2004	233.79

[1] Dobbs, M. M. 2017. Dragonflies and Damselflies (Odonata) of Georgia, the southeastern U.S., and beyond
  http://www.mmdragon.net/downloads/index.html

[2] Montgomery, E. B. YEAR. The distribution and relative seasonal abundance of Indiana species of five families of dragonflies (Odonata, Calopterygidae, Petaluridae, Cordulegasteridae, Gomphidae and Aeshnidae).

[3] LeGrand, H. E. and T. E. Howard, 2014. The dragonflies and damselflies of North Carolina. http://www.dpr.ncparks.gov/odes/a/accounts.php

[4] Barlow, A. and J. Bangma. 2006. Seasonal occurrence of the Odonates in New Jersey. http://njodes.org

[5] Smith-Patten, B. D., M. A. Patten, M. J. Dreiling, and J. Fisher. 2007. Phenology and new county records of Odonata of northeastern Oklahoma. Publications of the Oklahoma Biological Survey. 8: 1-13.

[6] Orr, R. L. 1996. The Odonata of Patuxent wildlife research center and vicinity. Bulletin of American Odonatolology 4: 37–67

[7] McShaffrey, D. 2009. Ohio Odonata Society http://w3.marietta.edu/~odonata/species/odolist.html

[8] Olcott, S. 2011. Final Report for the West Virginia dragonfly and damselfly atlas. West Virginia division of natural resources.

[9] Wagner, D. L., and M. C. Thomas. 1999. The odonatan fauna of Connecticut. Bulletin of American Odonatology. 5: 59-85.

[10] White, Erin L., Jeffrey D. Corser, and Matthew D. Schlesinger. 2010. The New York dragonfly and damselfly survey 2005 2009: Distribution and status of the Odonates of New York. New York Natural Heritage Program, Albany, New York. 424 pp.

[11] Blust, M. and B. Pfeiffer. 2015. The Odonata of Vermont. Bulletin of American Odonatology. 11: 69 - 119.

[12] Brunelle, P. M., and P. deMaynadier. 2005. The Maine damselfly and dragonfly survey: a final report.

Table S2. Sample size of common green darner (*Anax junius*) adults whose natal origins were assigned using stable-hydrogen isotopes captured in the hardiness zones (Hardiness Zone) used to summarize populations during each calendar month (Month).

Hardiness Zone	Month											
	Jan	Feb	Mar	Apr	May	Jun	Jul	Aug	Sep	Oct	Nov	Dec
7	0	0	5	45	53	74	52	10	7	3	0	0
8	0	0	2	14	45	65	53	16	3	1	0	0
9	0	0	1	12	22	20	67	8	0	1	0	0
10	0	2	14	23	27	12	17	4	3	1	0	0
11	8	10	45	27	13	11	13	10	8	3	7	7